Available online at www.CivileJournal.org

Civil Engineering Journal

(E-ISSN: 2476-3055; ISSN: 2676-6957)

Vol. 12, No. 06, June, 2026

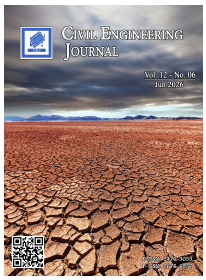

Numerical Investigation of Wave Transmission Characteristics Over Submerged Breakwater

Oki Setyandito [1*], Andrew John Pierre [1], Alfaldo B. Baria [1], Nizam [2], Martin Anda [3], Kevin Ardian Krisanto [1]

[1] *Civil Engineering Department, Bina Nusantara University, Jakarta 11480, Indonesia.*

[2] *Department of Civil and Environmental Engineering, Gadjah Mada University, Yogyakarta 55284, Indonesia.*

[3] *Environmental Engineering, Murdoch University, Western Australia 6150, Australia.*

Received 08 August 2025; Revised 21 April 2026; Accepted 05 May 2026; Published 01 June 2026

Abstract

This study presents a three-dimensional numerical investigation of wave transmission over submerged breakwaters, with a focus on elucidating the role of structural permeability in wave energy dissipation. High-resolution simulations were conducted using FLOW-3D and rigorously validated against laboratory measurements reported by van Gent et al. (2023). The results show that permeable submerged breakwaters consistently yield lower wave transmission coefficients than impermeable configurations due to enhanced internal turbulence and porous-flow energy dissipation mechanisms. Building on the validated numerical database, a refined empirical wave transmission model is developed. Compared to the widely used formulation of van Gent et al. (2023), the proposed model reduces the root mean square error from approximately 0.045 to 0.022 while maintaining a high coefficient of determination ($R^2 = 0.96$). The improvement is most pronounced for moderate to high relative freeboard conditions, where existing models tend to underestimate transmission. A comprehensive parametric analysis further quantifies the influence of crest width, relative freeboard, and porosity on transmission behavior. The key scientific contribution of this study lies in establishing a validated numerical–empirical framework that explicitly captures three-dimensional turbulence–porosity interactions, enabling faster and more accurate prediction of wave transmission and providing a scalable alternative to extensive physical modeling for the design of submerged and reef-type breakwaters.

Keywords: Submerged Breakwaters; Wave Transmission; FLOW-3D; Coastal Protection; Permeable Structures; Impermeable Structures.

1. Introduction

Climate change has exacerbated both the magnitude and frequency of coastal hazards, including sea level rise, changes in wave climate characteristics, and increased extreme water levels, posing significant risks to low-lying coastal areas around the world [1, 2]. These processes exacerbate wave-induced flooding, accelerate coastal erosion, and increase the vulnerability of coastal infrastructure, driving the need for coastal protection strategies that are not only hydraulically effective but also adaptive to long-term environmental change. Conventional coastal protection is dominated by hard engineering solutions such as seawalls, levees, and separate breakwaters designed to directly dampen wave energy. Although these structures have proven effective in reducing wave energy, their rigid nature is often associated with negative impacts on coastal landscape aesthetics, disruption of natural ecological and morphological

* Corresponding author: okisetyandito@binus.ac.id; osetyandito@binus.edu

https://doi.org/10.28991/CEJ-2026-012-06-022

processes, and limited flexibility in responding to increasingly dynamic hydrodynamic conditions due to climate change [3]. As a result, coastal engineering research and practice are gradually shifting toward more adaptive and environmentally oriented protection approaches.

Submerged wave breakers and artificial reef structures have emerged as promising alternatives, as they can reduce wave energy without obstructing the view of the sea, while also potentially providing additional ecological benefits through the creation of marine habitats [4, 5]. The reduction of wave energy by submerged structures is influenced by a combination of wave breaking, turbulence formation, internal flow through porous media, and partial wave reflection, which collectively reduce wave transmission toward the shoreline. Beyond their hydraulic function, permeable and reef-type structures are increasingly being considered within the framework of nature-based solutions or hybrid approaches, where coastal protection objectives are integrated with ecological enhancement and coastal morphological stability [6-8]. Wave transmission over submerged breakwaters has been extensively studied through laboratory experiments and empirical formulations. The classic empirical model generally relates the wave transmission coefficient to the key geometric and hydrodynamic parameters, such as relative freeboard, wave height and slope, crest width, and structure slope [9-11]. However, although these formulations are quite reliable for conventional impermeable or homogeneous breakwaters, their limitations become apparent when applied to structures with complex geometry, heterogeneous permeability, and significant internal flow mechanisms. As a result, the hydraulic performance of permeable submerged breakwaters, especially when compared to impermeable configurations, is still not well understood.

In this study, three dimensional numerical modeling is employed to analyze wave structure interactions, as such models can represent free surface deformation, wave breaking processes, internal flow through porous media, and localized energy dissipation mechanisms that are difficult to capture using simplified empirical approaches [12]. This research investigates the wave transmission characteristics of submerged breakwaters using a three-dimensional numerical model validated against laboratory experimental data reported by van Gent et al. (2023) [13]. Two configurations are considered: an impermeable trapezoidal submerged breakwater and a permeable submerged structure.

In addition to the comparative hydraulic evaluation, the validated numerical results are used to support a refinement of existing wave transmission coefficients, aiming to improve their predictive reliability under submerged and permeable conditions while remaining consistent with established empirical formulations. By applying identical wave conditions to both configurations, this study examines differences in wave transmission behavior and clarifies the role of permeability and internal flow in controlling wave energy dissipation mechanisms. Unlike previous studies that primarily rely on empirical formulations or standalone laboratory experiments, this work integrates three dimensional numerical modeling with laboratory validation, enabling more time and cost efficient assessments than physical laboratory modeling. The laboratory setup is explicitly reproduced within the numerical framework using FLOW-3D, ensuring a consistent and reliable basis for comparative analysis. The remainder of this paper is organized as follows. Section 2 presents the theoretical background of wave transmission coefficients, reviews existing empirical transmission models, and outlines the fundamental numerical formulation and computational approach employed in FLOW-3D [14].

2. Methodology

The research methodology is structured to evaluate the performance of submerged breakwaters in reducing and transmitting wave energy through an integrated numerical modelling approach, as shown in Figure 1.

At Point (1), the study begins with the definition of submerged breakwater configurations, consisting of impermeable and permeable structures with identical geometric dimensions and placement. This approach ensures that any observed differences in hydrodynamic response can be attributed solely to the effect of structural permeability.

At Point (2), numerical simulations are conducted within a two-dimensional wave flume domain, incorporating a wave-generation boundary at the upstream end and a wave absorber at the downstream end to minimize wave reflection. The submerged breakwater is positioned at a prescribed location within the domain, while several point probes are installed upstream and downstream of the structure to record temporal variations in free surface elevation.

At Point (3), the simulated free surface elevation is analyzed at selected time intervals to investigate wave transformation processes over the submerged breakwater, including shoaling, energy dissipation, and changes in wave propagation patterns.

The final stage, as presented at Point (4), involves the analysis of wave transmission by calculating the wave transmission coefficient (K_t) based on the ratio of transmitted to incident wave heights, followed by validation against available physical model data from previous experimental studies. This validation step is undertaken to assess the reliability of the numerical model in reproducing wave–structure interactions and to ensure the scientific robustness of the obtained results.

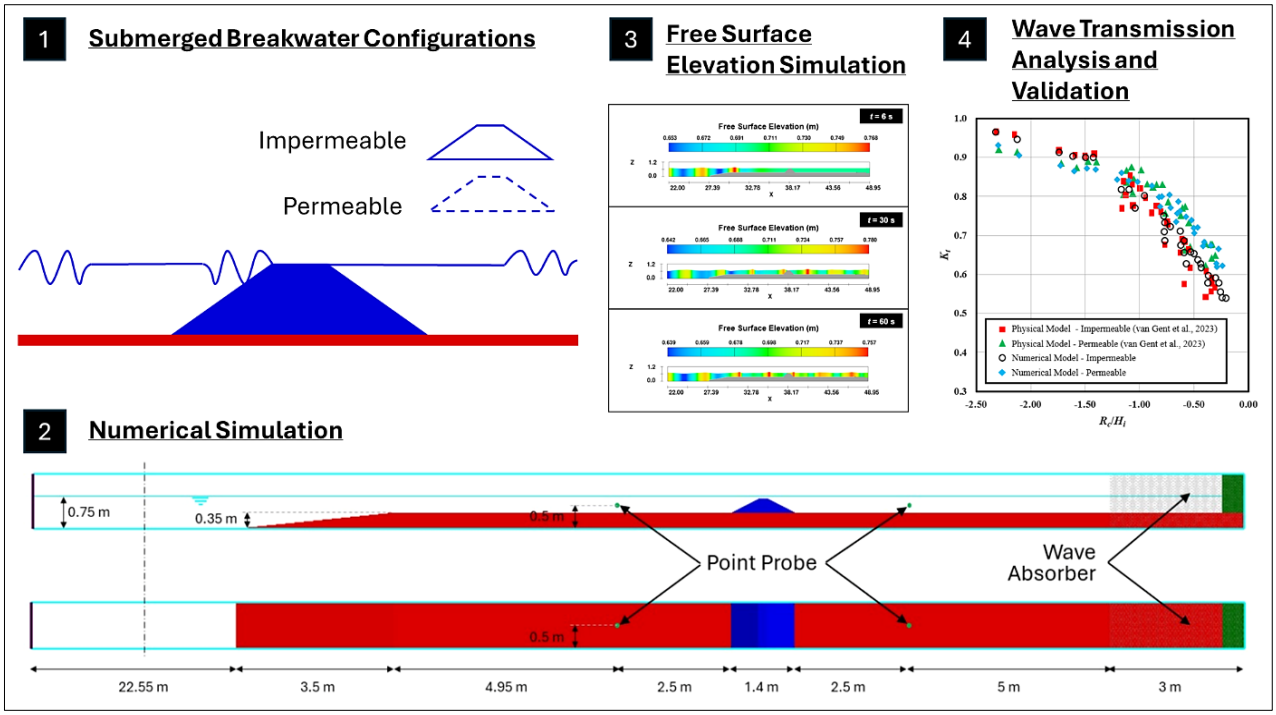

Figure 1. Numerical methodology framework for wave transmission analysis over submerged breakwaters

2.1. Fundamental Wave Theory and Energy Framework

Surface gravity waves propagating toward the coast act as the primary mechanism for energy transfer from offshore regions to the nearshore zone. Within the framework of linear wave theory, wave energy is composed of equal contributions of potential and kinetic energy. The depth-integrated, time-averaged wave energy per unit horizontal area can be expressed as Equation 1 [15]:

$$E = \frac{1}{8}\rho g H^2 \tag{1}$$

where, E denotes the wave energy, ρ is the water density, g is gravitational acceleration, and H represents the wave height. This relationship highlights that wave energy scales with the square of wave height, implying that relatively small changes in wave height may lead to substantial variations in wave energy. For irregular sea states, wave height is commonly represented by the spectral significant wave height $Hm_0 = 4\sqrt{m_0}$, where m_0 is the zeroth moment of the wave energy spectrum, a convention widely adopted in recent wave structure interaction studies [12, 13, 16].

When incident waves interact with a coastal structure, the redistribution of wave energy into reflected, transmitted, and dissipated components follows the principle of energy conservation. This energy balance is schematically shown in Figure 3 and formulated in Equation 2:

$$E_i = E_r + E_t + E_d \tag{2}$$

where, E_i is the incident wave energy, E_r is the reflected wave energy, E_t is the transmitted wave energy, and E_d represents the energy dissipated by the structure. This formulation provides the fundamental theoretical basis for analyzing wave transmission phenomena at coastal structures, including submerged and porous systems [13]. By normalizing Equations 3 and 4 with respect to the incident wave energy and invoking the quadratic relationship between wave energy and wave height, the energy balance can be expressed in dimensionless form as:

$$1 = \left(\frac{H_t}{H_i}\right)^2 + \left(\frac{H_r}{H_i}\right)^2 + \frac{E_d}{E_i} \tag{3}$$

which is commonly simplified as:

$$1 = {K_t}^2 + {K_r}^2 + {K_d}^2 \tag{4}$$

where, K_t, K_r, and K_d denote the wave transmission, reflection, and dissipation coefficients, respectively. This formulation explicitly illustrates that the reduction of wave energy behind a structure results from the combined effects of reflection and energy dissipation, while the transmitted component governs the residual wave climate in the lee of the structure.

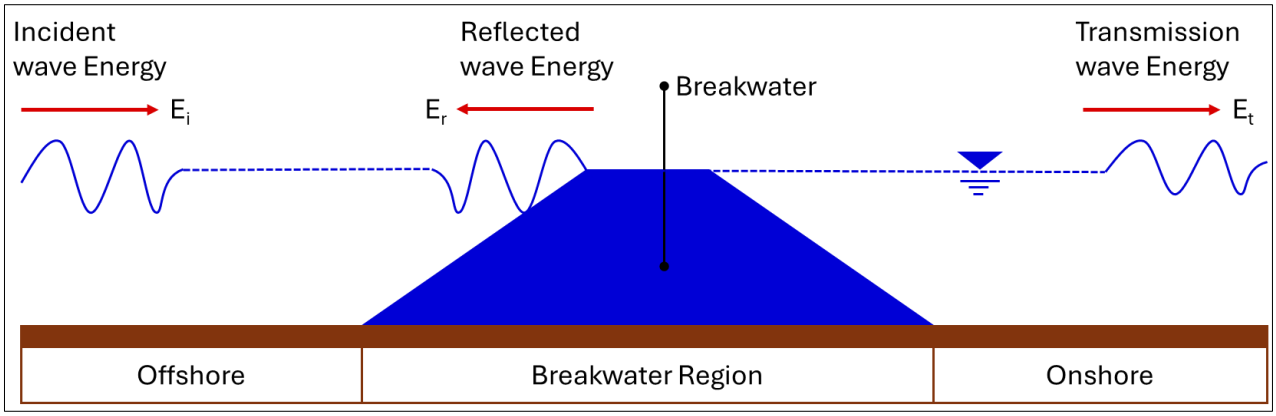

Figure 2. Schematic illustration of wave reflection, transmission, and energy dissipation over a submerged breakwater

2.2. Wave Transmission Fundamentals

Wave transmission through coastal structures is influenced by freeboard height (R_c), crest width (B), wave height (H_0), and wave steepness (s). Sollitt & Cross were among the first to correlate transmission coefficients to these parameters [17]. Daemen (1991) further introduced formulations for submerged and emerged rubble mound structures under irregular wave conditions [6,]. Submerged breakwaters and artificial reefs are increasingly favored in coastal protection due to their capability to attenuate wave energy while offering ecological co-benefits. The key parameter used to evaluate the hydraulic performance of such structures is the wave transmission coefficient (K_t), which is defined in Equation 5:

$$K_t = \left(\frac{H_t}{H_i}\right) \tag{5}$$

where, H_t is the transmitted significant wave height measured behind the structure and H_i is the incident significant wave height in front of the structure. The value of K_t is governed by several parameters: relative freeboard (R_c/H_i), crest width, structure porosity, slope, and wave conditions. While classical formulations provide general insight, they often fail to represent the complex, non-linear hydrodynamics occurring in reef-type or eco-engineered designs under submerged conditions [17, 18].

2.3. Empirical Models

To facilitate practical design, numerous empirical formulations have been proposed to estimate the wave transmission coefficient based on laboratory experiments. One of the earliest and still widely referenced models for submerged rubble-mound breakwaters is that proposed by Daemen [6], which is expressed in Equation 6 [13, 17]:

$$K_t = \left(0.031\frac{H_{m0}}{D_{n50}} - 0.024\right)\frac{R_c}{D_{n50}} + \left(0.51 - 5.42_{sop} + 0.0323\frac{H_{m0}}{D_{n50}} - 0.0017\left(\frac{B}{D_{n50}}\right)^{1.84}\right) \tag{6}$$

Among the most commonly applied formulations is the model developed by d'Angremond et al., which proposed a widely cited expression incorporating the surf similarity parameter ξ_{op}, as presented in Equation 7 [10].

$$K_t = 0.4\left(\frac{R_c}{H_0}\right) + c \cdot exp\left(0.5\xi_{op}\right)\left(\frac{B}{H_0}\right)^{0.31} \tag{7}$$

For wide-crested structures, modified versions of the original formulation have been proposed for large relative crest widths, applicable for $B/H_0 > 10$ and $B/H_0 > 12$, respectively. More recently, a comprehensive model incorporating effective width, porosity, local water depth, and a wave damping parameter ψ has been introduced, as presented in Equation 8 [13, 17].

$$K_t = 0.576\, ln\left(0.428(1 + cot\,\alpha)^{0.042}\left(1 + \frac{R_c}{H_0}\right)^{0.75}\left(\frac{B_{eff}}{D_{50}}\right)^{0.125}\left(\frac{L_P}{B_{eff}}\right)^{0.39}\omega^{0.413}\,\psi^{0.18}\right) + 0.923 \tag{8}$$

Despite their usefulness, these empirical formulations are constrained by the diversity of experimental methods and structural configurations employed in their derivation. A more recent study introduced a simplified empirical formulation for the wave transmission coefficient (K_t) applicable to submerged and reef-type breakwater structures, as expressed in Equation 9 [13]:

$$K_t = c_1 tanh\left(\frac{R_c}{H_i} + c_2\left(\frac{B}{L}\right)^{c_3} + c_4\right) + c_5 \tag{9}$$

This formulation integrates the effects of wave steepness and crest width through a single non-dimensional ratio B/L, where the spectral wavelength (L) is defined in Equation 10 [13]:

$$L = \frac{g}{2\pi}T^2 \tag{10}$$

The equation successfully captures the transmission behavior across various breakwater types, including impermeable, permeable, and perforated structures. However, several limitations have been identified. The model does not consider local water depth, structural porosity, or stone diameter, which although found to be negligible within the scope of their experimental range may exert significant influence under different structural configurations and environmental conditions. Furthermore, the formulation is derived solely from experimental data collected under partially submerged conditions ($2.5 < Rc/H_0 < 0$), offering limited applicability to emerged scenarios. It also lacks a specialized formulation for perforated structures, despite their complex and unique transmission characteristics. More recent empirical approaches for homogeneous porous submerged breakwaters have been proposed and subsequently validated against extensive experimental datasets, as expressed in Equation 11 [17, 18].

$$K_t = f\left(\frac{R_c}{H_{m0}}, \frac{B}{H_{m0}}, \xi_{op}, n\right) \tag{11}$$

These formulations demonstrate improved predictive capability for permeable structures, highlighting the growing importance of internal structural parameters in controlling wave transmission. In response to these limitations, the present study seeks to enhance the empirical modeling approach by incorporating a broader range of validation through both numerical and physical simulations, particularly for perforated breakwaters and a wider spectrum of environmental settings. This refinement is expected to yield a more representative and practically applicable formulation of K_t contributing to the advancement of coastal structure design practices.

2.4. FLOW-3D RANS–VOF Numerical Framework for Wave Transmission Analysis

FLOW-3D is employed in this study to overcome the inherent limitations of conventional empirical formulations, which often oversimplify wave–structure interactions by neglecting internal hydrodynamics, turbulence effects, and nonlinear flow behavior, particularly in submerged and porous coastal structures [19, 20]. By solving the three-dimensional Reynolds-Averaged Navier–Stokes (RANS) equations coupled with the Volume of Fluid (VOF) method for free-surface tracking and the RNG $k-\varepsilon$ turbulence closure, FLOW-3D provides a robust, physics-based numerical framework capable of resolving wave transformation and energy dissipation processes within complex porous media [13, 21]. Mass conservation is enforced through the continuity equation, as expressed in Equation 12:

$$\frac{\partial \rho}{\partial t} + \nabla.(\rho u) = 0 \tag{12}$$

where, ρ represents the fluid density and u denotes the three-dimensional velocity vector of the flow, ensuring consistent balance between temporal density variations and spatial mass fluxes in wave-induced flows [14, 19]. Momentum transport is governed by the RANS formulation, as expressed in Equation 13:

$$\frac{\partial \rho u}{\partial t} + \nabla.(\rho u) = -\nabla P + \mu\nabla^2 u + Pg \tag{13}$$

in which P is the hydrodynamic pressure, μ denotes the dynamic viscosity of the fluid, and g is the gravitational acceleration vector, allowing the combined effects of inertia, viscous diffusion, pressure gradients, and gravity to be consistently represented in three-dimensional wave–structure interaction problems [19, 20]. A key advantage of FLOW-3D lies in its integrated porous media formulation, where the hydraulic resistance of rubble-mound and reef-type structures is introduced as an additional volumetric force term in the momentum equations using the Darcy–Forchheimer approach [20]. This resistance force is expressed in Equation 14:

$$F_p = -\left(\frac{\mu}{K}u + C_{F\rho}|u|u\right) \tag{14}$$

where, F_p denotes the resistance force per unit volume acting within the porous medium, K is the effective permeability, and C_F is the inertial resistance coefficient accounting for nonlinear flow effects at higher velocities. Within this homogenized framework, the influence of stone size distribution is incorporated implicitly through the macroscopic resistance parameters rather than resolved at the particle scale, an approach that has been shown to be effective for engineering-scale wave transmission analysis [22]. From an energetic perspective, wave dissipation within the porous structure is governed by the cumulative hydraulic resistance acting on the flow as it propagates through the porous medium. This integrated resistance controls the reduction of wave energy between the incident and transmitted sides of the structure and therefore determines the wave transmission coefficient, defined as the ratio of transmitted to incident wave heights. As a result, the global wave transmission behavior is primarily controlled by macroscopic parameters such as structural porosity, thickness, and relative submergence, whereas the influence of local stone-size heterogeneity

remains secondary [13, 16]. FLOW-3D supports a wide range of wave conditions, including regular, irregular, and user-defined wave inputs, together with flexible boundary conditions that closely replicate laboratory and field configurations. The numerical outputs, such as velocity fields, pressure distributions, turbulence quantities, and free-surface elevations, enable direct investigation of key physical processes including flow separation, vortex formation, and turbulence intensification around the structure crest and within the porous core, which play a critical role in governing wave transmission behavior [23].

The RNG $k-\varepsilon$ turbulence model is selected due to its improved performance under high strain rates and strong streamline curvature typical of submerged breakwaters. Within the RANS framework, turbulence effects are represented using an eddy-viscosity approach, where the turbulent viscosity is defined in Equation 15:

$$\mu_t = \rho C_\mu \frac{k^2}{\varepsilon} \tag{15}$$

where, μ_t denotes the turbulent (eddy) viscosity, k represents the turbulent kinetic energy, ε is the rate of turbulent kinetic energy dissipation, and C_μ is a model constant. Compared to the standard $k-\varepsilon$ model, the RNG formulation introduces an analytical correction to the dissipation equation, leading to improved prediction of energy dissipation in highly sheared and curved flows. Comparative studies indicate that although Large Eddy Simulation (LES) is capable of resolving finer turbulence structures, the RNG $k-\varepsilon$ model provides comparable accuracy in predicting bulk wave transmission behavior at a substantially lower computational cost [24, 25]. Furthermore, differences among RANS turbulence closures have been shown to exert a secondary influence on wave transmission coefficients when compared with the dominant effects of geometric and hydraulic parameters of the structure, such as porosity, thickness, and relative submergence [26, 27]. Accordingly, the RANS approach employing the RNG $k-\varepsilon$ turbulence model is considered appropriate for the present study, which focuses on the efficient and reliable prediction of wave transmission over submerged and porous breakwaters.

3. Results

This study employs a three-dimensional flume to simulate wave transmission across two seperate submerged coastal structures: an impermeable trapezoidal structure and a permeable rubble mound breakwater. The numerical framework is developed to replicate key aspects of the physical simulation setup by van Gent et al. (2023) [13], enabling a direct comparison between numerical predictions and actual occurences observed in the physical simulation. The simulations were conducted using FLOW-3D with the Reynolds-Average Navier-Stokes (RANS) equations in combination with the Volume of Fluid (VOF) method to capture the dynamic evolution of the fluid interface. In this study, the Renormalization Group (RNG) $k-\varepsilon$ turbuence model was selected to resolve turbulence effects, particularly instigated by wave breaking, flow seaparation, and dissipation within and around the structures. The numerical wave flume configuration, including the breakwater structures, point probes, and wave absorber zones, is illustrated in Figure 3, providing a visual reference for the simulation setup in FLOW-3D.

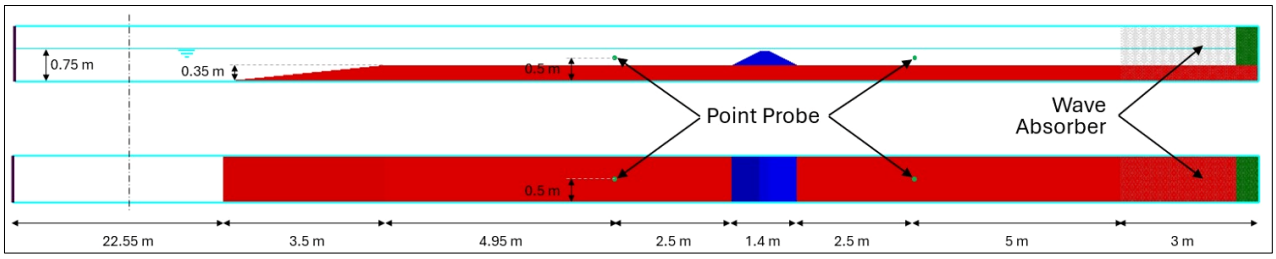

Figure 3. Simulation setup in FLOW-3D: Numerical wave flume configuration with breakwater structure, point probes, and wave absorber zones

The computational domain was configured to replicate the physical wave flume employed in the experimental study by van Gent et al. (2023) [13]. The domain has a total length of 110 m, a width of 1 m, and a height of 1.2 m, with a still water depth of 0.75 m. The seabed topography consists of a 13.9 m long horizontal platform connected to the foreshore through a 1:10 sloping ramp, providing a smooth transition from the offshore region to the nearshore area. This geometric configuration ensures close consistency between the numerical model and the experimental setup, thereby enabling meaningful comparison of hydraulic responses. The numerical simulations were performed using FLOW-3D with a structured Cartesian mesh of uniform size 0.1 m, resulting in a total of 32,400 computational cells within the main mesh block. The adopted mesh resolution represents a compromise between numerical accuracy and computational efficiency and is consistent with established practices in RANS–VOF-based numerical wave tank modeling. Initial fluid regions, boundary conditions, and other simulation parameters were explicitly defined to ensure stable wave generation and propagation prior to wave structure interaction. A detailed summary of the computational setup, including boundary conditions and numerical options, is provided in Table 1.

Table 1. FLOW-3D simulation parameter

Parameter	Value/option
Mesh size	0.1 m (cartesian mesh)
Total calculated cells for mesh block	32400 cells
Turbulence model	RNG Model; maximum turbulent mixing length for RANS models were dynamically computed.
Fluid region initial condition	x_{min} = 4 m; x_{max} = 170 m y_{min} = -5 m; y_{max} = 5 m z_{min} = 0 m; z_{max} = 7 m
Boundary condition	x_{min}= Wave; x_{max} = Wall y_{min} = Symmetry; y_{max} = Symmetry z_{min} = Wall; z_{max} = Pressure
Wave generator	Type: 5th order Stokes-Fenton

Wave generation was implemented using the fifth-order Stokes–Fenton wave theory available in FLOW-3D, which accurately represents nonlinear wave kinematics for the simulated wave steepness range (s=0.015–0.03). Free-surface elevations were recorded using stationary point probes located 2.5 m upstream and downstream of the structure to consistently extract incident and transmitted wave parameters, following established numerical practice [13, 17]. The free surface was captured using the Volume of Fluid (VOF) method with a split-Lagrangian scheme, which is well established for nonlinear wave propagation and wave–structure interaction problems [13, 19]. A uniform mesh size of 0.1 m was adopted as a compromise between numerical accuracy and computational efficiency. Previous CFD studies have demonstrated that global wave parameters, including transmitted wave height, converge at comparable grid resolutions, while further refinement mainly affects local flow details [18, 22]. Preliminary mesh refinement tests confirmed that reducing the grid size resulted in changes in transmitted wave height of less than 3 %, indicating that the selected mesh is adequate for the objectives of this study.

Porous media properties were represented using a single effective stone diameter based on a Darcy–Forchheimer formulation. This macroscopic approach has been shown to capture the dominant hydraulic response of rubble-mound structures, as wave transmission is primarily governed by bulk porosity and characteristic stone size rather than detailed grain-size heterogeneity [20]. Recent studies further indicate that stone-size variability mainly influences local turbulence and internal flow structures, with limited impact on global transmission coefficients [13]. To minimize artificial wave reflection, a downstream damping zone was applied with a gradually increasing damping coefficient. The effectiveness of this approach was verified by monitoring free-surface elevations near the outlet, confirming negligible reflected wave amplitudes relative to the incident wave height. Similar damping strategies have been shown to reliably reduce numerical reflection and ensure accurate transmission measurements in nonlinear numerical wave tanks [26-28].

Figure 4 illustrates the geometrical profile of the submerged breakwater structure adopted in the FLOW-3D numerical simulations. The modeled configuration represents a trapezoidal submerged breakwater, which is widely used in coastal protection applications due to its hydraulic efficiency and structural stability. Two structural conditions are considered in this study, namely impermeable breakwaters, representing conventional solid or concrete-type structures, and permeable breakwaters, which simulate rubble-mound or porous artificial reef-type systems that allow partial wave energy dissipation through internal flow. The Table 2 presents the variations in the simulation setup for wave transmission through submerged coastal structures. It includes different parameter combinations such as the structure's slope (S), crest freeboard (R_c), incident wave height (H_0), and wave period (T_0). These variations are essential for analyzing the impact of different design conditions on wave transmission performance, providing a comprehensive overview of how structural and hydrodynamic factors influence wave behavior in coastal environments.

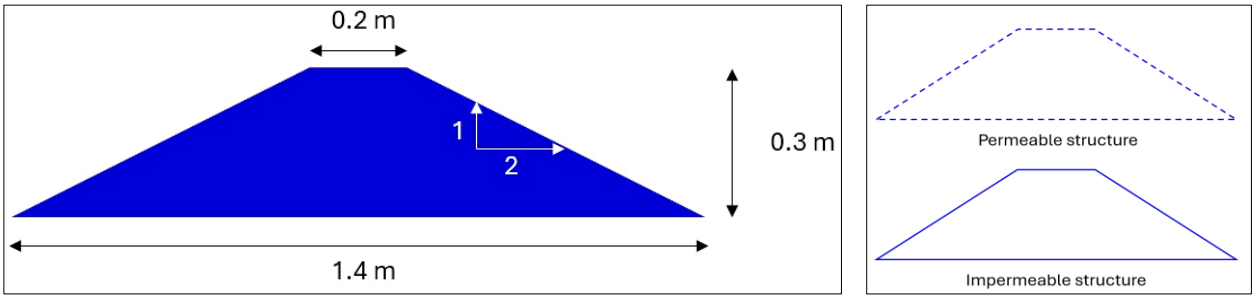

Figure 4. Geometrical profile of the submerged breakwater structure used in FLOW-3D simulations

Table 2. Simulation Setup Variations for Wave Transmission

Case	S	D (m)	R_c	H_0 (m)	T_0 (m)
1	0.015	0.35	-0.05	0.1	2.07
2	0.015	0.4	-0.1	0.1	2.07
3	0.015	0.45	-0.15	0.1	2.07
4	0.015	0.5	-0.2	0.1	2.07
5	0.015	0.35	-0.05	0.15	2.53
6	0.015	0.4	-0.1	0.15	2.53
7	0.015	0.45	-0.15	0.15	2.53
8	0.015	0.5	-0.2	0.15	2.53
9	0.015	0.35	-0.05	0.2	2.92
10	0.015	0.4	-0.1	0.2	2.92
11	0.015	0.45	-0.15	0.2	2.92
12	0.015	0.5	-0.2	0.2	2.92
13	0.015	0.35	-0.05	0.25	3.27
14	0.015	0.4	-0.1	0.25	3.27
15	0.015	0.45	-0.15	0.25	3.27
16	0.015	0.5	-0.2	0.25	3.27
17	0.03	0.35	-0.05	0.1	1.46
18	0.03	0.4	-0.1	0.1	1.46
19	0.03	0.45	-0.15	0.1	1.46
20	0.03	0.5	-0.2	0.1	1.46
21	0.03	0.35	-0.05	0.15	1.79
22	0.03	0.4	-0.1	0.15	1.79
23	0.03	0.45	-0.15	0.15	1.79
24	0.03	0.5	-0.2	0.15	1.79
25	0.03	0.35	-0.05	0.20	2.07
26	0.03	0.4	-0.1	0.20	2.07
27	0.03	0.45	-0.15	0.20	2.07
28	0.03	0.5	-0.2	0.20	2.07
29	0.03	0.35	-0.05	0.25	2.31
30	0.03	0.4	-0.1	0.25	2.31
31	0.03	0.45	-0.15	0.25	2.31
32	0.03	0.5	-0.2	0.25	2.31

3.1. Simulation of Free Surface Elevation over an Submerged Breakwater

Figure 5 illustrates the temporal evolution of free surface elevation for both impermeable and permeable submerged breakwater configurations, highlighting the contrasting hydrodynamic responses induced by structural permeability. In this study, the impermeable breakwater was modeled as a rigid, non-porous trapezoidal body with 1:2 side slopes, a crest width of 0.20 m, and a total height of 0.30 m. The structure was defined as a smooth solid with a no-slip boundary condition and zero internal porosity, allowing the analysis to focus exclusively on geometric effects on wave transformation mechanisms. Figure 5-a presents the free surface elevation profiles at three representative time instances (t = 6 s, 30 s, and 60 s). The horizontal axis (x) denotes the longitudinal flume direction, while the vertical axis (z) represents the water surface elevation. At t = 6 s, the incoming wave front begins interacting with the breakwater, resulting in an upstream increase in surface elevation due to partial reflection. As the simulation advances to t = 30 s, wave shoaling and reflection intensify, leading to pronounced deformation of the wave crest and increased spatial variability in free surface elevation. By t = 60 s, the wave field approaches a quasi-steady state, characterized by a dynamic balance between incident, reflected, and transmitted wave components, with attenuated oscillations observed downstream of the structure. Similar reflection-dominated behavior for impermeable submerged breakwaters has been widely reported in both experimental and numerical studies [13, 17].

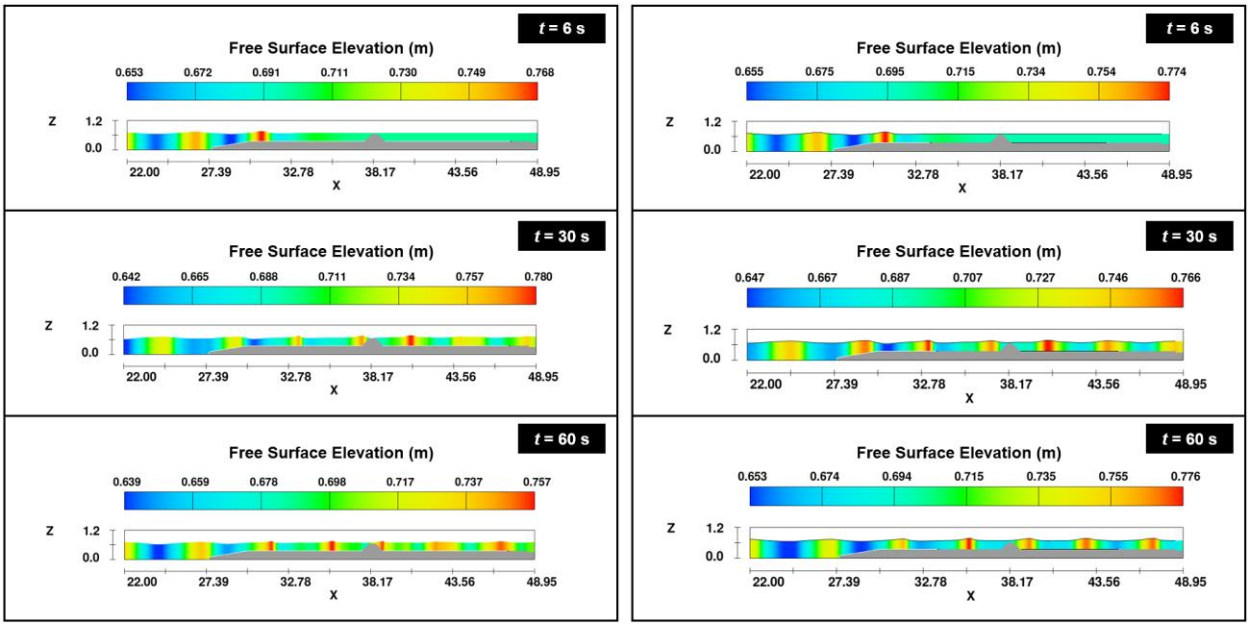

(a) (b)

Figure 5. Result of free surface elevation on (a) impermeable and (b) permeable structure at different time intervals

Conversely, the permeable breakwater configuration shown in Figure 5-b allows fluid exchange through the porous matrix, facilitating additional dissipation of wave energy via internal drag forces and turbulence generation. Compared to the impermeable case, the permeable structure exhibits reduced peak free surface elevations and smoother spatial gradients, indicating enhanced wave attenuation and diminished transmitted wave energy. This behavior is consistent with established findings that demonstrate a strong dependence of wave transmission and deformation on structural porosity, where increased permeability leads to higher energy dissipation and lower transmission coefficients [22, 29]. Experimental investigations have demonstrated that permeable submerged breakwaters yield lower transmission coefficients and higher energy loss relative to non-porous counterparts under comparable wave conditions, attributable to enhanced internal energy dissipation within the porous medium. Numerical studies employing porous-media approaches further support these observations, showing that internal flow resistance and turbulence within permeable structures play a critical role in controlling wave transformation processes. The present numerical results therefore align well with existing literature, reinforcing the effectiveness of permeable submerged breakwaters in attenuating wave energy through combined geometric and porosity-induced dissipation mechanisms [13, 22].

3.2. Simulation of Velocity Over a Submerged Breakwater

Figure 6 shows the velocity magnitude distribution around submerged structures for (a) an impermeable configuration and (b) a permeable configuration at t = 6 s, 30 s, and 60 s. As illustrated in Figure 6-a, the impermeable structure generates higher velocity magnitudes near the crest and in the downstream region, indicating strong flow acceleration and wave reflection due to minimal energy dissipation. In contrast, Figure 6-b demonstrates that the permeable structure significantly reduces velocity intensity and produces smoother flow patterns, as wave energy is dissipated within the porous medium. These numerical results are consistent with established findings on wave transmission and flow attenuation at low-crested and porous coastal structures [9, 10], thereby confirming the reliability of the present model in capturing the key hydrodynamic mechanisms governing wave structure interactions.

Figures 7 and 8 present the time histories of fluid velocity magnitude measured upstream and downstream of the submerged breakwater (BW) over the interval t = 10–60 s for impermeable and permeable configurations, respectively. As shown in Figure 7, the velocity signal recorded before the impermeable breakwater exhibits higher peak values and stronger oscillations, reflecting the dominance of incident wave energy with minimal attenuation. Conversely, the velocity measured after the structure shows a marked reduction in both peak magnitude and fluctuation amplitude, indicating effective dissipation of wave-induced momentum. This pronounced attenuation is mainly associated with wave breaking, flow separation, and energy losses caused by the solid geometry of the impermeable breakwater. In comparison, Figure 8 demonstrates that the permeable submerged breakwater also reduces downstream velocity levels; however, residual oscillations remain evident, suggesting partial wave transmission through the porous medium. The observed behavior highlights the role of permeability in allowing controlled energy passage while promoting dissipation via turbulence generation and internal friction within the structure. Overall, the contrasting responses between impermeable and permeable configurations are consistent with established numerical and experimental studies on wave transmission and velocity attenuation by submerged and low-crested breakwaters [10, 13, 17], thereby confirming the capability of the present numerical framework to reliably capture the key hydrodynamic mechanisms governing flow attenuation across submerged coastal protection structures.

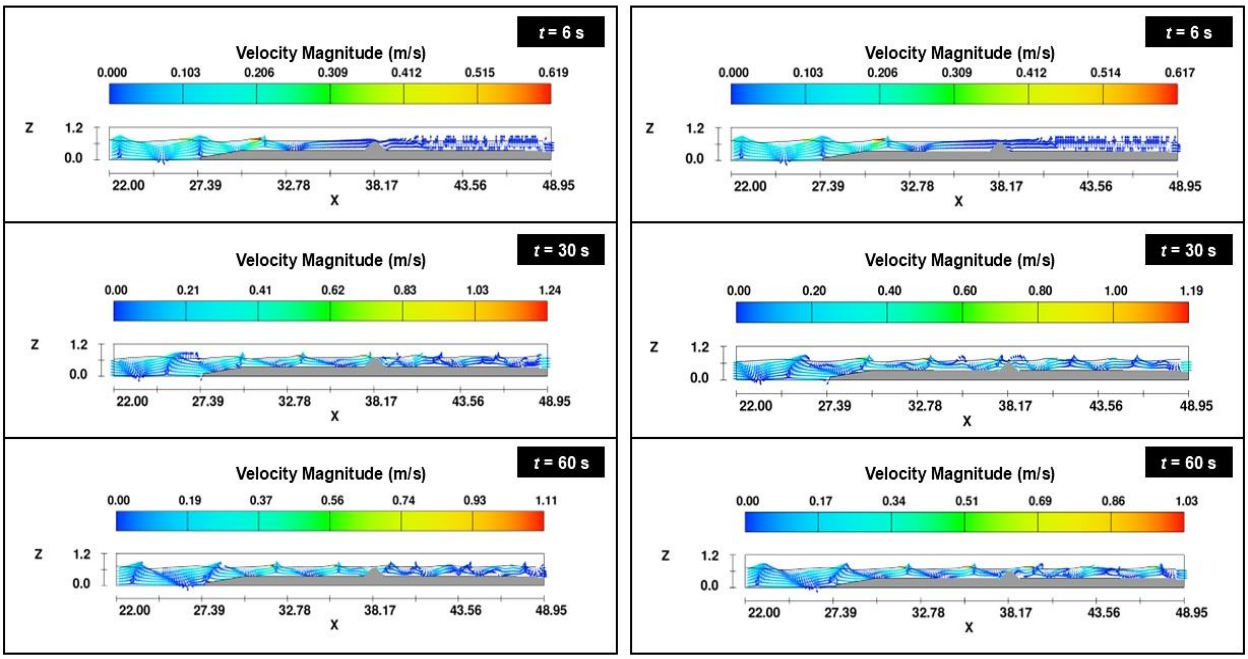

(a) (b)

Figure 6. Velocity magnitude distribution around submerged structures at different time instants: (a) impermeable structure and (b) permeable structure

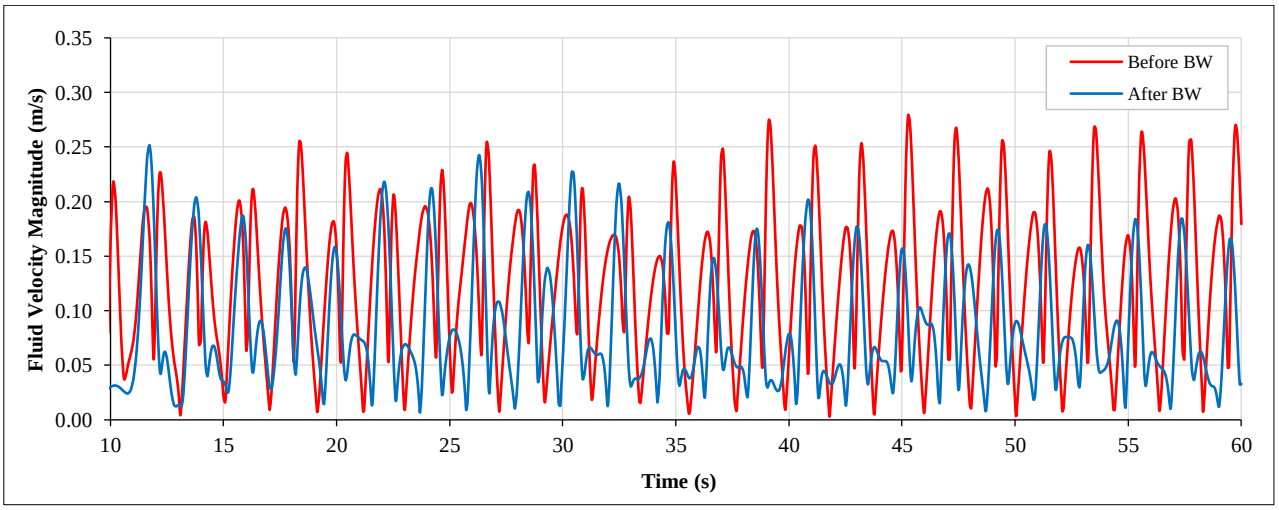

Figure 7. Time series of fluid velocity magnitude before and after the impermeable submerged breakwater (BW)

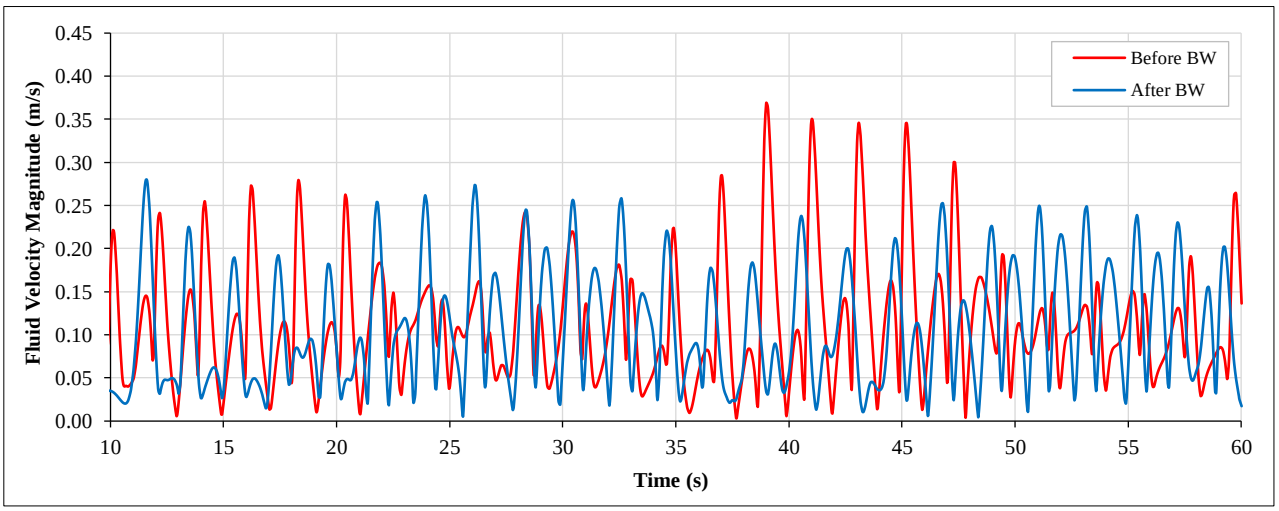

Figure 8. Time series of fluid velocity magnitude before and after the permeable submerged breakwater (BW)

3.3. Permeable Rubble Mound Structure

The permeable structure was modelled as a porous zone using FLOW-3D's porosity media model. A homogeneous trapezoidal geometry with the same outer dimensions as Model A was defined. The porosity was set to n = 0.436, based on an effective stone diameter D_{50} = 0.04 m, calculated using Darcian saturated drag equation. Figure 5-b presents a simulation of the free surface elevation for a permeable structure breakwater at different time intervals: 6 seconds, 30 seconds, and 60 seconds, using FLOW-3D.

The simulation illustrates how the water surface elevation (in meters) changes along the horizontal axis (x), with the vertical axis (z) representing the water depth. At t = 6 s, the wave movement is initially observed, with surface elevation gradually increasing across the structure. By t = 30 s, the surface elevation continues to evolve, showing more pronounced variations in the wave patterns along the x-axis. At t = 60 s, the surface elevation begins to stabilize, but still shows some fluctuations along the length of the breakwater. The color gradient in the plots represents different elevation levels, helping to highlight the dynamic nature of the waves and their interaction with the permeable breakwater structure over time. This simulation provides valuable insights into how water interacts with a permeable structure, which is crucial for coastal engineering and breakwater design assessments.

Surface elevation series were recorded at the virtual probes located upstream and downstream of the structures. The wave transmission coefficient, K_t was calculated by comparing the average wave heights over a steady-state period (H_t/H_i). To provide further insight into the hydraulic performance and submergence effects of the structures the non-dimensional freeboard ratio, R_c/H_i was also computed. The numerical results were then validated to the computed transmission coefficients and the non-dimensional freeboard ratio against the physical model data from van Gent et al. (2023) [13]. Both trend and magnitude confirmed the reliability of the FLOW-3D simulations for modelling wave-structure interaction for both impermeable and permeable breakwater configurations as illustrated in the Figure 9.

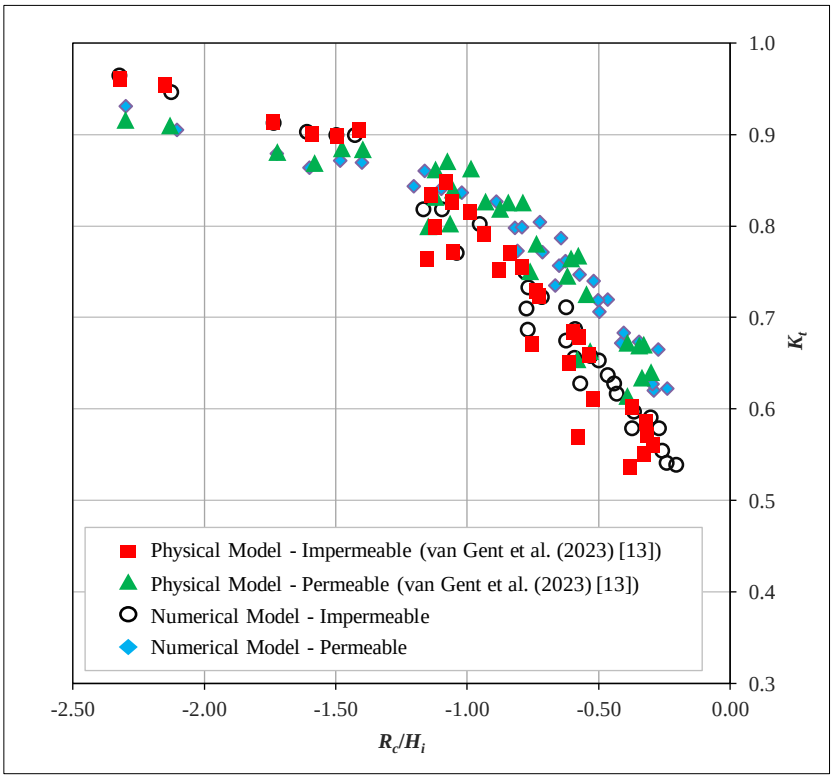

Figure 9. Comparison of measured and simulated wave transmission coefficients for permeable and impermeable breakwaters

3.4. Analysis of Test Results

The numerical model was validated against physical model test results to ensure the accuracy and reliability of the simulation. A strong agreement was observed between the numerically simulated wave transmission coefficients (K_t) and those obtained from experimental measurements shown in Figure 10. The trends exhibited by the numerical data closely follow the physical test results, indicating that the numerical approach successfully captures the wave

transmission behavior across various configurations. The minor deviations observed are within acceptable limits, confirming the credibility of the numerical model for further parametric and design analysis.

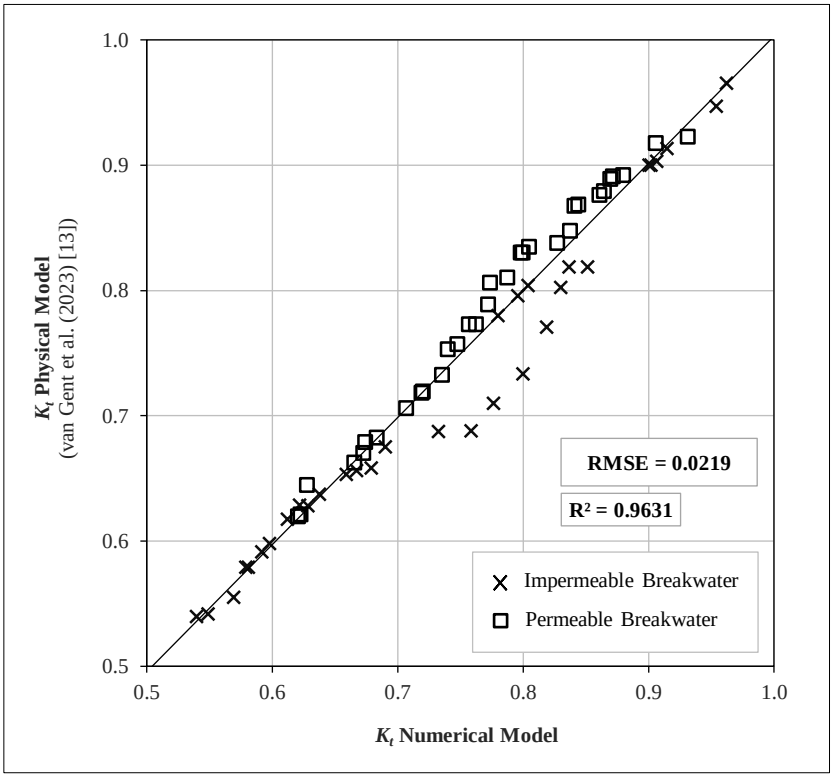

Figure 10. Comparison between numerical and physical model results for wave transmission coefficient K_t: assessment of van gent et al. (2023) [13] model accuracy

Figure 10 presents a comparison between the wave transmission coefficients (K_t) obtained from a numerical model and those measured through physical model testing as reported by Van Gent et al. (2023) [13]. The data include both impermeable and permeable breakwater structures, represented by cross and square markers, respectively. The close alignment of the data points along the 1:1 reference line indicates a strong agreement between the numerical and physical models. The very low Root Mean Square Error ($RMSE$) of 0.0219 and high coefficient of determination (R^2 = 0.9631) further confirm the reliability and predictive accuracy of the numerical simulations. This high level of correlation validates the numerical model as a robust tool for simulating wave transmission through both types of breakwaters. The consistency with previously published experimental data provides a solid foundation for extending the numerical analysis to broader parametric studies or engineering applications, especially in conditions where physical modeling may be limited or infeasible [13].

Following the validation, a regression analysis was conducted on the numerical results to establish empirical relationships between the transmission coefficient (K_t) and the relative crest freeboard parameter (R_c/H_i), defined as the ratio of structure crest elevation to the incident wave height. An exponential function was adopted as the fitting model:

$$K_t = a \,.\, e^{R_c/H_0} + b \tag{16}$$

For the impermeable structure, the curve-fitting process yielded coefficients of a = –0.610 and b = 1.017, as shown in Figure 11. The graph demonstrates that K_t decreases exponentially with decreasing R_c/H_i, indicating that higher crest elevations relative to the wave height significantly reduce wave transmission. In contrast, the permeable structure exhibited a slightly different trend. The fitted parameters for the permeable case were a = –0.437 and b = 0.980, as illustrated in Figure 12. While the exponential behavior remains, the slope is gentler compared to the impermeable structure, reflecting the role of internal energy dissipation due to the material porosity. This additional damping mechanism affects the transmission coefficient, particularly at lower crest freeboard values.

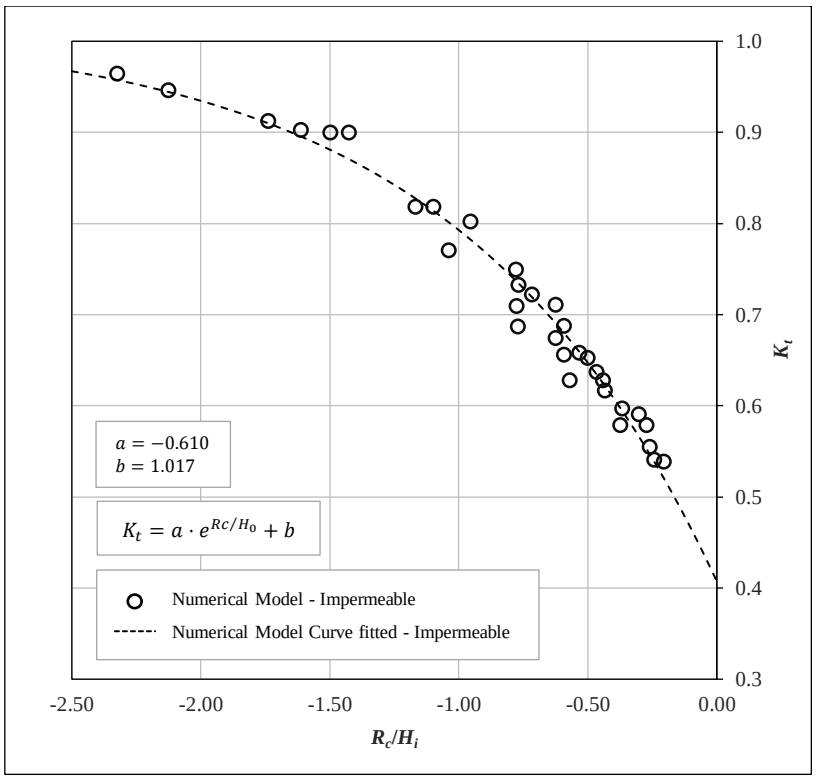

Figure 11. Comparison between numerical and physical model results for wave transmission coefficient K_t: assessment of van Gent et al. (2023) [13] model accuracy

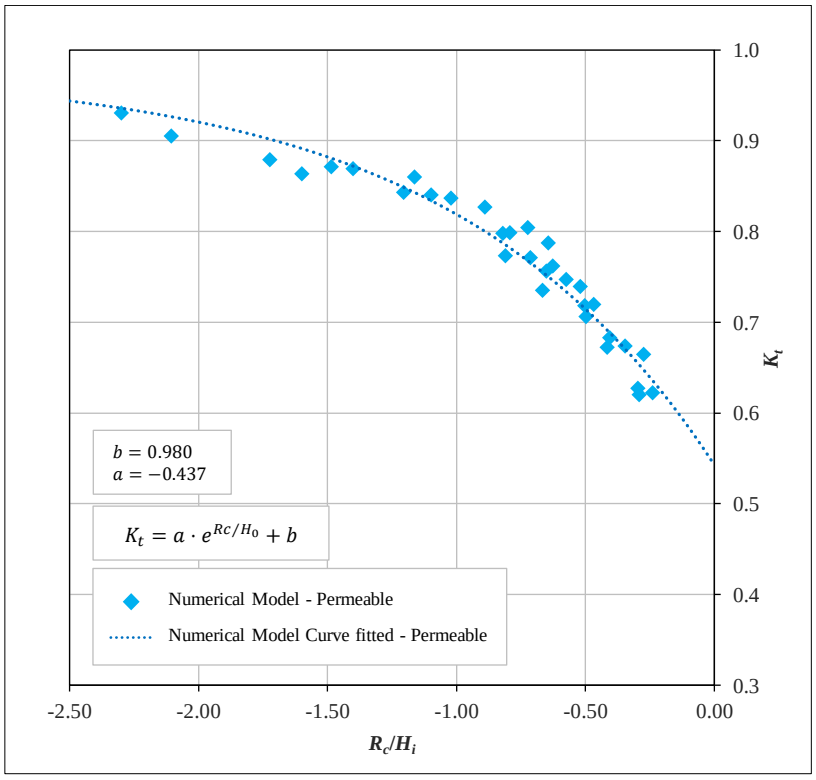

Figure 12. Curve fitting of wave transmission over permeable breakwaters based on relative freeboard: an exponential model approach

These fitted empirical models not only confirm the accuracy of the numerical simulations but also provide practical predictive tools for estimating wave transmission under varying design conditions. The exponential relationships developed for both impermeable and permeable breakwaters can be utilized in preliminary design and optimization of coastal defense structures, offering a balance between hydraulic performance and structural feasibility.

Figure 13 presents an integrated comparison of Figures 11 and 12, which individually illustrate the exponential regression curves for impermeable and permeable breakwater structures, respectively. This combined representation enables a direct comparative analysis of the wave transmission coefficient (K_t) as a function of the relative crest freeboard (R_c/H_i) across both structural configurations. By consolidating the two datasets into a single plot, the figure enhances clarity in observing the differing trends in wave energy attenuation behavior and facilitates a more comprehensive interpretation of the hydrodynamic performance associated with each breakwater type.

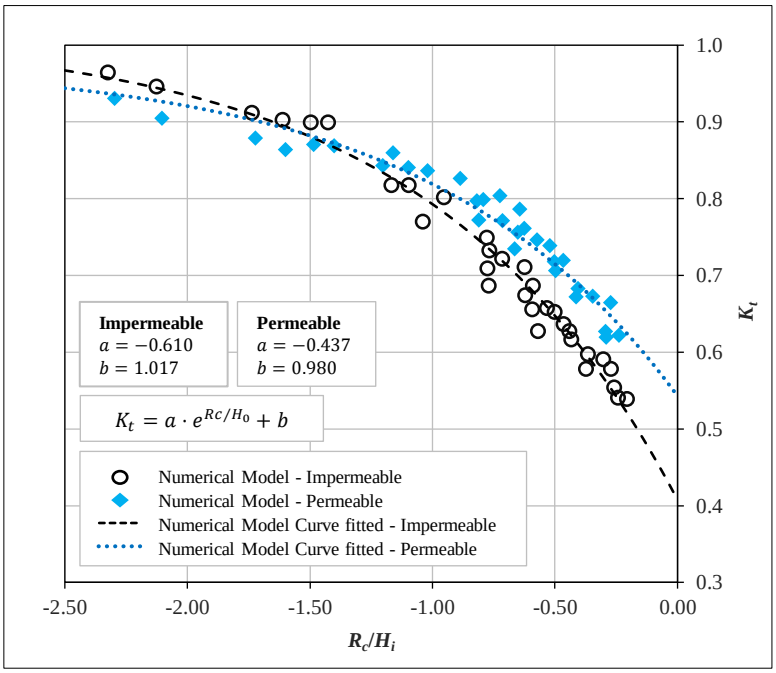

Figure 13. Exponential curve fitting of wave transmission coefficient K_t based on relative freeboard R_c/H_0 of impermeable and permeable breakwaters

Figure 14 presents a comparison between the wave transmission coefficients (K_t) calculated using the proposed curve-fitted empirical formula (horizontal axis) and those obtained from FLOW-3D numerical simulations (vertical axis). Each data point represents a pair of predicted and simulated values under identical structural and wave conditions. The data points cluster closely along the 1:1 reference line ($K_{t\ calculated} \approx K_{t\ calculated}$),demonstrating a strong agreement between the empirical model and the numerical results with regression R^2 = 0.9654

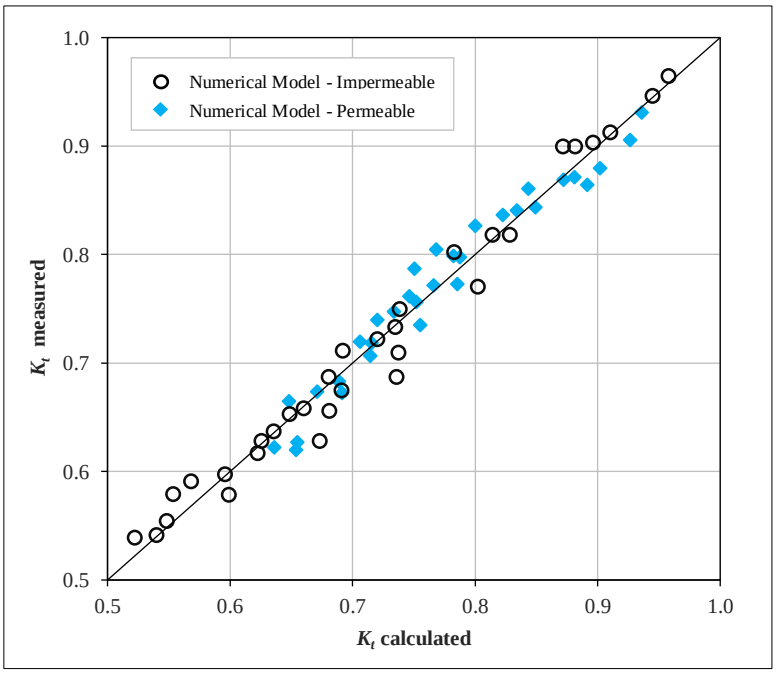

Figure 14. Validation of the exponential transmission model through measured and calculated K_t comparison for impermeable and permeable breakwaters

Figure 15 represents the data points cluster closely along the 1:1 reference line ($K_{t\ calculated} \approx K_{t\ calculated}$), demonstrating a strong agreement between the empirical model and the numerical results with regression R^2 = 0.9654. This close alignment indicates that the curve-fitted formula reliably reproduces the physical behavior of wave transmission in permeable submerged rubble mound structures. The consistency observed in this comparison validates the empirical formula as a reliable approximation. It also supports its potential for further development to accommodate a wider range of structural conditions, such as varying porosity, material size distribution, and relative submergence.

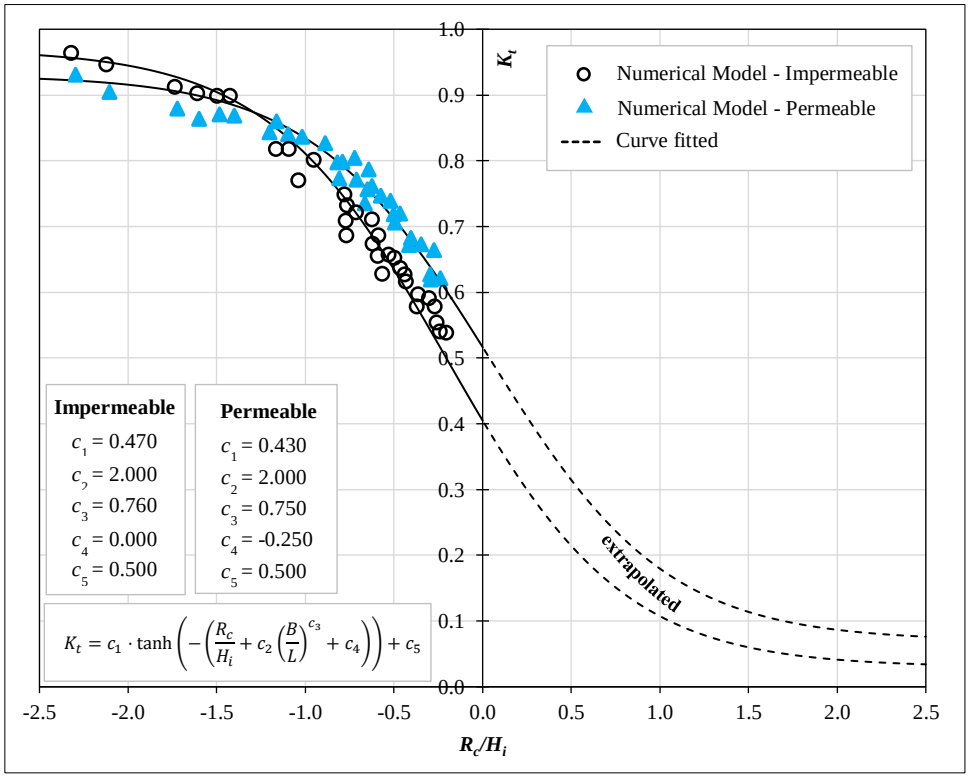

Figure 15. Hyperbolic tangent curve fitting of the empirical wave transmission model for permeable and impermeable breakwaters

To improve the predictive accuracy of wave transmission across submerged coastal structures particularly those incorporating porous configurations, an enhanced empirical formulation has been proposed. This model extends the classical framework of Equation 9 by optimizing its calibration coefficients through nonlinear regression techniques. The wave transmission coefficient, K_t is defined as a function of key hydrodynamic and geometric parameters, including the crest freeboard (R_c) incident wave height (H_i), crest width (B), and wavelength (L) A set of empirical coefficients c_1, c_2, c_3, c_4, and c_5 are systematically calibrated to align with results obtained from high fidelity numerical simulations. This refinement enhances the model's capability to capture both linear and nonlinear wave-structure interactions, thereby providing a more robust and accurate representation of wave transmission behavior in complex submerged porous systems (see Table 3).

Table 3. Empirical Calibration Coefficients

Coefficient	Impermeable Structure	Permeable Structure
c_1	0.470	0.430
c_2	2.000	2.000
c_5	0.760	0.750
c_4	0.000	-0.250
c_5	0.500	0.500

Compared to the reference model proposed by Van Gent et al. (2023) [13], the current formulation introduces an additional degree of freedom in the calibration process and integrates permeability effects through the c_4 correction term. While the Van Gent model captures general trends using a simplified polynomial or logarithmic form, it may fail to represent the more nuanced dissipation behaviors found in permeable structures. The proposed model addresses this limitation by incorporating exponential decay and saturation behavior via the tanh function, which constrains K_t within a realistic physical range between 0 and 1. The effectiveness of this advanced empirical model is visually demonstrated in Figure 10, where numerical results for permeable structures (represented by blue triangular markers) are plotted

against the fitted curve (dashed line). The close agreement between the model prediction and the numerical data validates the robustness of the proposed formulation across a wide range of relative crest freeboard and structural width-to-wavelength ratios. Particularly in the transitional region where partial transmission and overtopping coexist, the model captures the nonlinearity more accurately than previous formulations.

4. Conclusion

This study provides a comprehensive numerical analysis of submerged breakwaters, with a specific focus on the hydraulic performance of impermeable and permeable structures. The numerical simulations conducted using FLOW-3D, validated by experimental data, demonstrate that submerged breakwaters are highly effective in mitigating wave transmission. Notably, permeable structures exhibit superior performance relative to impermeable ones, owing to their enhanced capacity for energy dissipation through internal flow dynamics and turbulence. These findings substantiate the potential of permeable submerged breakwaters as an effective solution for reducing wave energy and enhancing coastal protection.

In addition to these significant findings, this research introduces a refined empirical model that advances the accuracy of predictions for wave transmission across submerged breakwaters. The proposed model improves upon existing formulations, particularly the one by van Gent et al. (2023) [13], by incorporating more complex factors that influence wave-structure interactions. The study further emphasizes the importance of key design parameters, such as crest width, freeboard, and porosity, in optimizing both hydraulic efficiency and structural performance. These parameters are shown to play a crucial role in the wave attenuation capabilities of submerged breakwaters, with permeable structures offering the added advantage of ecological co-benefits, which aligns with the principles of sustainable coastal defense. While the results of this study are promising, it is important to acknowledge certain limitations, particularly with respect to the scalability of the numerical models and their sensitivity to environmental variations. These factors point to the need for further refinement of the models to enhance their applicability to a broader range of real-world coastal environments. Future research should focus on addressing these limitations, particularly in terms of the real-world variability of environmental conditions and the adaptation of models to diverse coastal scenarios. This study makes a substantial contribution to the field of coastal engineering by advancing the understanding of submerged breakwater performance and providing valuable insights for the design of more efficient, sustainable, and multifunctional coastal defense systems. The results offer a strong foundation for future research and the practical application of submerged breakwaters in coastal protection, contributing to the growing body of knowledge on nature-based solutions in coastal engineering.

5. Declarations

5.1. Author Contributions

Conceptualization, O.S. and N.N.; methodology, O.S. and A.J.P.; software, A.J.P. and A.B.B.; validation, O.S. and N.N.; formal analysis, O.S., M.A., and N.N.; investigation, O.S. and A.J.P.; resources, O.S.; data curation, A.J.P. and A.B.B.; writing—original draft preparation, O.S. and A.J.P.; writing—review and editing, M.A., K.A.K., and N.N.; visualization, A.J.P. and K.A.K.; supervision, O.S.; project administration, A.B.B. and K.A.K.; funding acquisition, O.S. and N.N. All authors have read and agreed to the published version of the manuscript.

5.2. Data Availability Statement

The data presented in this study are available on request from the corresponding author.

5.3. Funding and Acknowledgement

This research has been partially funded by Bina Nusantara University and Research Grant from Ministry of Higher Education, Science and Technology, Indonesia. The authors duly acknowledge the support from both institutions, without which this research could not have been done.

5.4. Conflicts of Interest

The authors declare no conflict of interest.

6. References

[1] Field, C., Fischlin, A., Fitzharris, B. B., Gay García, C., Hanson, C., Harasawa, H., Hennessy, K., Huq, S., Jones, R., Kajfež Bogataj, L., Karoly, D., Klein, R.,…. (2007). Coastal systems and low-lying areas. Climate Change 2007: Impacts, Adaptation and Vulnerability. Contribution of Working Group II to the Fourth Assessment Report of the Intergovernmental Panel on Climate Change, Cambridge University Press, Cambridge, United Kingdom.

[2] Rueda, A., Vitousek, S., Camus, P., Tomás, A., Espejo, A., Losada, I. J., Barnard, P. L., Erikson, L. H., Ruggiero, P., Reguero, B. G., & Mendez, F. J. (2017). A global classification of coastal flood hazard climates associated with large-scale oceanographic forcing /704/106/829/2737 /704/4111 /141 /129 article. Scientific Reports, 7(1), 5038. doi:10.1038/s41598-017-05090-w.

[3] Ben-Natan, A., & Shashar, N. (2025). A Short Review of Strategies for Augmenting Organism Recruitment on Coastal Defense Structures. Journal of Marine Science and Engineering, 13(1), 95. doi:10.3390/jmse13010095.

[4] Morris, R. L., Konlechner, T. M., Ghisalberti, M., & Swearer, S. E. (2018). From grey to green: Efficacy of eco-engineering solutions for nature-based coastal defence. Global Change Biology, 24(5), 1827–1842. doi:10.1111/gcb.14063.

[5] Brancasi, A., Leone, E., Francone, A., Scaravaglione, G., & Tomasicchio, G. R. (2022). On Formulae for Wave Transmission at Submerged and Low-Crested Breakwaters. Journal of Marine Science and Engineering, 10(12), 1986. doi:10.3390/jmse10121986.

[6] Daemen, I. F. R. (1991). Wave Transmission at Low-Crested Structures. University of Technology, Delft Hydraulics, Delft, The Netherlands.

[7] Wang, Y., Wu, Y., Liu, Q., & Wang, X. (2023). Nature-based Solutions (NbS) Habitat Design Practices and Technical Measures for Urban Waterfront Areas. Journal of Civil Engineering and Urban Planning, 5(12), 67-72. doi:10.23977/jceup.2023.051210.

[8] Cohn, J. L., Copp Franz, S., Mandel, R. H., Nack, C. C., Brainard, A. S., Eallonardo, A., & Magar, V. (2022). Strategies to work towards long-term sustainability and resiliency of nature-based solutions in coastal environments: A review and case studies. Integrated Environmental Assessment and Management, 18(1), 123–134. doi:10.1002/ieam.4484.

[9] Van Der Meer, J. W., Briganti, R., Wang, B., & Zanuttigh, B. (2005). Wave Transmission at Low-Crested Structures, Including Oblique Wave Attack. Coastal Engineering 2004, 4152–4164. doi:10.1142/9789812701916_0335.

[10] d'Angremond, K., Van Der Meer, J. W., & De Jong, R. J. (1997). Wave Transmission at Low-Crested Structures. Coastal Engineering 1996, 2418–2427. doi:10.1061/9780784402429.187.

[11] Goda, Y., & Ahrens, J. P. (2009). New Formulation of Wave Transmission Over and Through Low-Crested Structures. Coastal Engineering 2008, 3530–3541. doi:10.1142/9789814277426_0293.

[12] Demirbilek, Z., Nwogu, O. G., Ward, D. L., & Sánchez, A. (2009). Wave transformation over reefs: Evaluation of one-dimensional numerical models. No. ERDCCHLTR091, U.S. Army Engineer Research and Development Center, Vicksburg, United States.

[13] van Gent, M. R. A., Buis, L., van den Bos, J. P., & Wüthrich, D. (2023). Wave transmission at submerged coastal structures and artificial reefs. Coastal Engineering, 184, 104344. doi:10.1016/j.coastaleng.2023.104344.

[14] Flow Science, Inc. (2008). User Manual FLOW-3D. Flow Science, Inc, Pasadena, United States.

[15] Memmola, F., Contestabile, P., Falco, P., & Brocchini, M. (2024). Test Reference Year for wave energy studies: Generation and validation. Renewable Energy, 224, 120169. doi:10.1016/j.renene.2024.120169.

[16] Le Xuan, T., Vu, H. T. D., Oberle, P., Dang, T. D., Tran Ba, H., & Le Manh, H. (2024). Hydrodynamics and wave transmission through a hollow triangle breakwater. Estuarine, Coastal and Shelf Science, 302, 108765. doi:10.1016/j.ecss.2024.108765.

[17] Sollitt, C. K., & Cross, R. H. (1972). Wave transmission through permeable breakwaters. Coastal Engineering 1972, 1827-1846. doi:10.1061/9780872620490.106.

[18] Kurdistani, S. M., Tomasicchio, G. R., D′Alessandro, F., & Francone, A. (2022). Formula for wave transmission at submerged homogeneous porous breakwaters. Ocean Engineering, 266, 113053. doi:10.1016/j.oceaneng.2022.113053.

[19] Hirt, C. W., & Nichols, B. D. (1981). Volume of fluid (VOF) method for the dynamics of free boundaries. Journal of Computational Physics, 39(1), 201–225. doi:10.1016/0021-9991(81)90145-5.

[20] Jensen, B., Jacobsen, N. G., & Christensen, E. D. (2014). Investigations on the porous media equations and resistance coefficients for coastal structures. Coastal Engineering, 84, 56–72. doi:10.1016/j.coastaleng.2013.11.004.

[21] Feichtner, A., Mackay, E., Tabor, G., Thies, P. R., Johanning, L., & Ning, D. (2021). Using a porous-media approach for CFD modelling of wave interaction with thin perforated structures. Journal of Ocean Engineering and Marine Energy, 7(1), 1–23. doi:10.1007/s40722-020-00183-7.

[22] Setyandito, O., Aslami, M. H., Anda, M., & Kristanti, R. A. (2023). Wave transmission at low-crested structures. E3S Web of Conferences, 429. doi:10.1051/e3sconf/202342902008.

[23] Yuniardi, R., Istiyanto, D. C., Wulandari, I., Harita, Y. T. D., Firmansyah, R., & Rachman, R. A. (2025). Comparison of Laminar, RNG, and LES Model for Wave Propagation Simulation with FLOW-3D. Journal of Geoscience, Engineering, Environment, and Technology, 10(3), 288–294. doi:10.25299/jgeet.2025.10.3.13933.

[24] Zhang, C., & Buldakov, E. (2025). Evaluating RANS and LES turbulence models in hybrid wave modelling of breaking waves. Frontiers in Marine Science, 12. doi:10.3389/fmars.2025.1484783.

[25] Linh, L. C., & Tri, M. C. (2023). Evaluating the performance of the RANS turbulence models for simulating wave propagation over a submerged breakwater using openfoam. Journal of Science and Technology in Civil Engineering (STCE) - HUCE, 17(1), 79–93. doi:10.31814/stce.nuce2023-17(1)-07.

[26] Didier, E., & Teixeira, P. R. F. (2022). Validation and Comparisons of Methodologies Implemented in a RANS-VoF Numerical Model for Applications to Coastal Structures. Journal of Marine Science and Engineering, 10(9), 1298. doi:10.3390/jmse10091298.

[27] Min, E. H., Koo, W., & Kim, M. H. (2023). Wave Characteristics over a Dual Porous Submerged Breakwater Using a Fully Nonlinear Numerical Wave Tank with a Porous Domain. Journal of Marine Science and Engineering, 11(9), 1648. doi:10.3390/jmse11091648.

[28] Huang, J., Lowe, R. J., Ghisalberti, M., & Hansen, J. E. (2024). Wave transformation across impermeable and porous artificial reefs. Coastal Engineering, 189, 104488. doi:10.1016/j.coastaleng.2024.104488.

[29] Jaffar Sidek, F., & Abdul Wahab, M. A.-J. (2018). the Effects of Porosity of Submerged Breakwater Structures on Non-Breaking Wave Transformations. Malaysian Journal of Civil Engineering, 19(1), 15744. doi:10.11113/mjce.v19.15744.